ACS OMEGA

http://pubs.acs.org/journal/acsodf
Article

Genesis and Accumulation Mechanism of Low-Rank CBM: A Case Study in the Jiergalangtu Block of Erlian Basin, Northern China

Ling Li, Dazhen Tang,* Hao Xu, Qin Meng, Haitao Lin, and Haipeng Yao

Cite This: *ACS Omega* 2024, 9, 1827−1837

ABSTRACT: In order to elucidate the origin of coalbed methane (CBM) in the Jiergalangtu block of Erlian Basin, Inner Mongolia of China, gas components, stable isotope tests of 22 gas samples, radioisotope dating measurements, and water quality analysis of 15 coproduced water samples were evaluated. On account of the geochemical data and genetic indicators, including C_1/C_{1-n}, $C_1/(C_2 + C_3)$, and $CO_2/(CO_2 + CH_4)$ (CDMI) values, $\delta^{13}C(CO_2)$, $\Delta\delta^{13}C_{(CO_2-CH_4)}$, $\delta^{15}N$, and $^3He/^4He$ combined with vitrinite reflectance (Ro) (0.29−0.48%, avg. 0.35%) of Saihantala formation, the results indicate that methane in the Jiergalangtu block is mostly dominated by primary and secondary biological gas, 40.91% of the gas samples are secondary biogas and primary biogas accounts for 59.19%. Among them, methyl-type fermentation accounts for 31.82%, and carbon dioxide (CO_2) reduction makes up 68.18%. CO_2 reduction generally occurs region-wide but is mainly associated with the central part of the block, where CO_2 depletion and ^{13}C enrichment take place correspondingly. Methane and CO_2 $\delta^{13}C$ almost tend to isotopically light along the margin of the block, indicating that gas generation is significantly affected by the methyl-type fermentation pathway. Meanwhile, the genesis analysis of other gas components in CBM is also investigated, CO_2 is mainly the associated product of microbial methanogenesis, and nitrogen (N_2) is primarily from the atmosphere with a little amount from the earth's crust. Furthermore, the formation time of coalbed water has been dissected based on the hydrogeochemical properties of the coproduced water samples. The coalbed water exhibit a $Na-HCO_3$ and $Na-HCO_3-Cl$ type and have a total dissolved solid (TDS) value ranging from 2458.58 to 5579.1 mg/L, with an average of 3440.55 mg/L. Moreover, comprehensive analysis of $\delta D(H_2O)$, $\delta^{18}O(H_2O)$, $\delta^{13}C_{DIC}$, and the radioisotope dating index [^3H, $^{14}C(Fm)$ and $^{14}C(BP)$] indicates that the coalbed water was formed in the Quaternary Pleistocene and rarely replenished by the present surface water. The mechanism of CBM accumulation is basically sorted out by synthesizing the history of burial, heat, and hydrocarbon generation. The CBM formation can be divided into four stages. That is, microbial gas production approximately began at the beginning of the Early Cretaceous and reached the peak of thermogenic gas production in the middle and late Early Cretaceous. At the end of the Early Cretaceous, strata possibly began to uplift, and denudation led to gas escape. From Neogene to Pleistocene, glacial meltwater tended to penetrate into coalbed on a large scale, and N_2 and CO_2 also entered the coal seams, stimulating abundant secondary biological gas generation. Since Holocene, geological conditions including temperature and TDS have become hostile to biogas generation, and biogas generation tends to stop. Therefore, the Jiergalangtu block mainly represents sealed primary biological gas and secondary biological gas in CBM reservoirs.

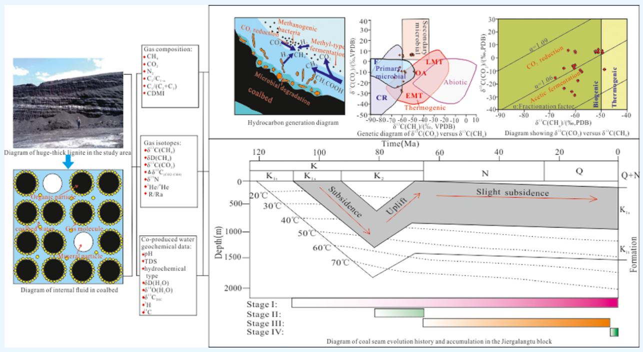

1. INTRODUCTION

Research on coalbed methane (CBM) genesis is an important part of the CBM accumulation mechanism.[1,2] CBM genesis can be divided into organic, inorganic, and mixed gas, among which organic gas includes primary biological gas, secondary biological gas, thermal degradation gas, and thermal cracking gas.[3,4] Based on geochemical indicators including gas composition and hydrocarbon isotopes and classical natural gas identification charts, biological gas has been identified in medium and low-rank coal bearing basins such as Powder River Basin, San Juan Basin, and Black Warrior Basin in the United States, Surat Basin in Australia, and Junggar Basin, Erlian Basin, Hailaer Basin, and Ordos Basin in China.[5−16] As a key field of CBM exploration and development in China, low-rank CBM has abundant resources but low gas content and low development degree. However, biological gas provides the main gas source supplement, which is expected to lay the

Received: October 27, 2023
Revised: November 20, 2023
Accepted: December 4, 2023
Published: December 18, 2023

https://doi.org/10.1021/acsomega.3c08490
ACS Omega 2024, 9, 1827−1837

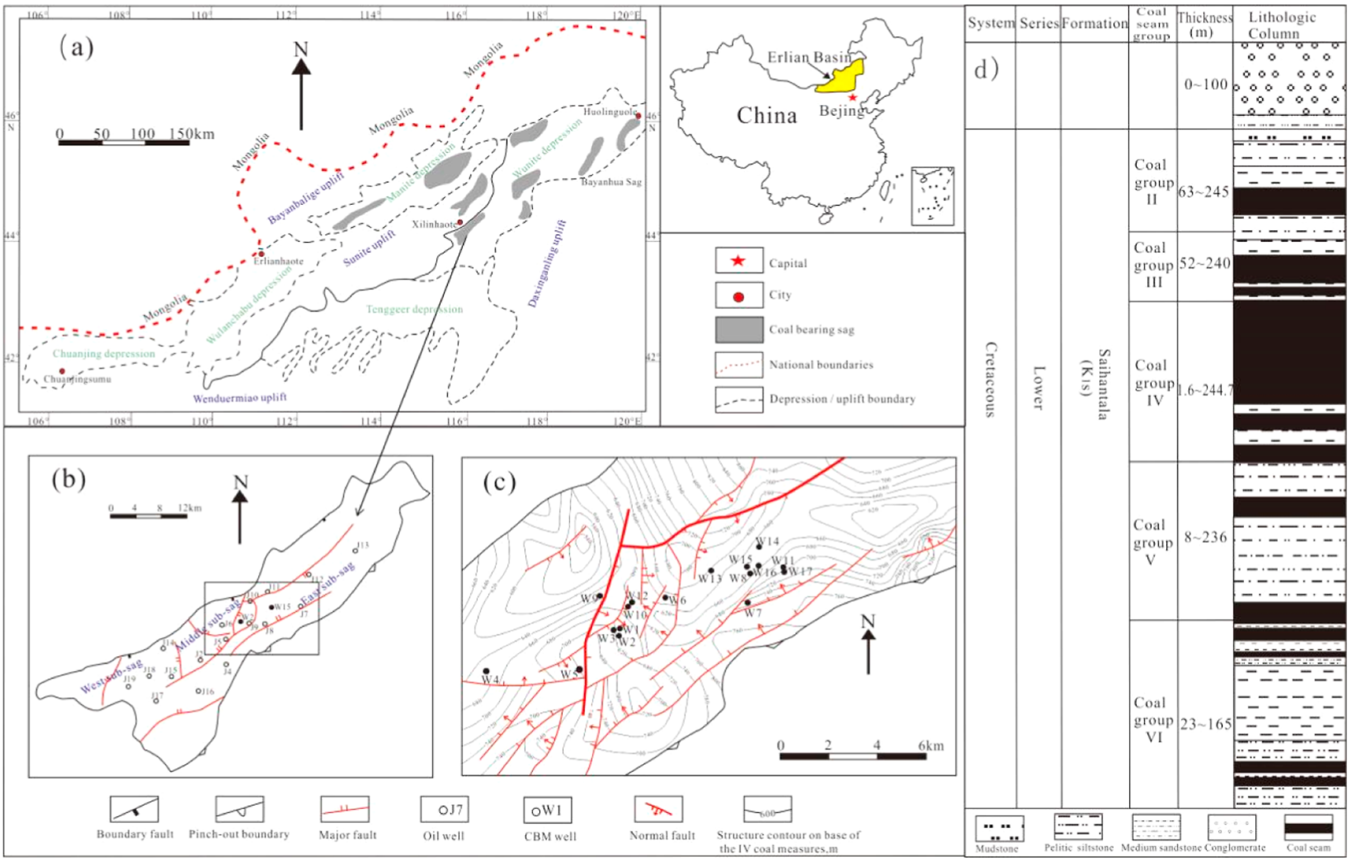

Figure 1. (a) Location map of the study area in Erlian Basin. (b) Map of the Jiergalangtu sag structural outline. (c) Map of the Jiergalangtu block structural outline and structural contour map of the base of the no. IV coal group. (d) Stratigraphic column of Cretaceous coal-bearing strata in the Jiergalangtu sag.

resource foundation for China's low-rank CBM to reserve growth and production addition.[17−22]

Jiergalangtu sag is a typical low-rank CBM field in the Early Cretaceous, which is located in the southwest margin of the Wunite Depression in the Erlian Basin. The study area is characterized by the development of shallow burial, ultrathick lignite, and the CBM resources reach probably 900 × 10^8 m^3.[23] As the first representative area in China to achieve a major breakthrough in CBM exploration in low-rank coal, the Jiergalangtu sag is currently in the pilot phase of large-scale development. 40 CBM wells have been constructed in the block by October 2023, with 10 wells exceeding 1000 m^3 per day. At present, the maximum single well production of vertical wells is 3007 m^3 per day, and that of horizontal wells is 4000 m^3 per day. However, most wells exhibit an unsatisfactory gas production effect. In order to determine the reasons for the production capacity differentiation, it is necessary to deepen the research on the genesis mechanism of CBM in addition to systematic elucidation of the geological control conditions for the gas content and the exploration and development links including drilling, fracturing, and drainage. The study of CBM genesis is of great significance for deepening the formation mechanism, evaluating the CBM resources, and analyzing the productivity differences.[12,21]

In recent years, research studies on CBM in the Jiergalangtu sag have mainly focused on sedimentation, reservoir physical properties, and enrichment rules;[24−31] however, the research studies on the genesis of CBM in this region is scarce. In this paper, combined with the results of the predecessors, representative gas samples and coproduced water samples of the CBM wells in the study area were collected to dissect gas components, isotope characteristics of the CBM, and geochemical characteristics of coalbed water. The genesis of CBM and gas reservoir types will be discussed, the enrichment law of the secondary biologic gas will be revealed, and the formation mechanism of CBM will be further clarified in the study area. It is expected to provide certain theoretical support for the exploration and development of a low-rank CBM in the Jilgarangtu block and even Erlian Basin.

2. GEOLOGICAL BACKGROUND

The Jiergalangtu sag is located at the southwest end of the Wunite Depression in Erlian Basin, which is an asymmetrical graben-shaped structure whose axis is near the northwest margin (Figure 1a). The sag was obviously transformed by the squeezing stress of the southeast-northwest with a dip of 0−12° and orientation of NE (Figure 1b). The study area is located in the center of the Jiergalangtu sag, of which the faults are relatively developed, mainly for normal faults, which have a certain destructive effect on the preservation of CBM (Figure 1c). CBM is presently produced mostly from coalbeds in the Lower Cretaceous Saihantala formation in the Jiergalangtu sag (Figure 1d). The Saihantala formation is composed of six coal groups in the Jiergalangtu sag, including 15 coal seams. The main coal groups consist downward of no. II, no. III, no. IV, no. V, and no. VI coalbeds. The roof and floor of coal groups are mudstone and silty mudstone (Figure 1d). The coal seams are mainly characterized by shallow burial and ultrathick. The

https://doi.org/10.1021/acsomega.3c08490
ACS Omega 2024, 9, 1827−1837

Table 1. Gas Components and Isotopic Compositions of CBM from CBM Production Wells in the Jiergalangtu Block

well name	depth/m	gas component/%				stable isotope/‰				$^3He/^4He$ (10^{-7})	$C_1/(C_2 + C_3)$	CDMI /%	C_1/C_{1-n}
		N_2	CH_4	C_{2+}	CO_2	$\delta^{13}C_{C_1}$	$\delta^{13}C_{CO_2}$	δD_{C1}	$\delta^{15}N$				
W1	547.76	8.86	85.67	0.13	5.34	−60.7	−9.2	−276.8			659.00	5.87	0.998
W2	505	8.15	88.76	0.26	2.83	−56.9	−10.6	−254			341.38	3.09	0.997
W3	364.8	4.95	91.62	0	3.43	−64.2	−23.1	−265			9162.00	3.61	1.000
W4	300	21.56	74.73	0.02	3.69	−60.4	−29.4	−218			3736.50	4.71	1.000
W5	367.3	3.12	91.9	0.38	4.6	−62.5	6.2	−275			241.84	4.77	0.996
W6	491.2	2.08	94.1	0.12	3.7	−60.3	5.3	−270.2			784.17	3.78	0.999
W7	615.6	1.59	94.2	0.11	4.1	−60.1	5.1	−270.8			856.36	4.17	0.999
W8	418	9.93	88.9	0	1.17	−68.5	−15.5	−265			8890.00	1.30	1.000
W9	340	15.12	82.22	0	2.66	−61	−26.7	−216			8222.00	3.13	1.000
W10	460	7.63	89.98	0.04	2.39	−48.7	−9.8	−176	−1.1	2.1	2249.50	2.59	1.000
W11	480	14.8	81.36	0.11	3.84	−51.5	4.2	−173.9	−1.2	1.54	739.64	4.51	0.999
W12	468	2.43	91.21	0.03	6.36	−50.8	6.8	−198.5	−3.6	1.68	3040.33	6.52	1.000
W13	487	10.4	86.46	0.12	3.14	−49.8	4	−185.9	−0.6	0.42	720.50	3.50	0.999
W14	480	3.43	93.46	0.11	3.1	−50.8	4.2	−190.2	−1.3	1.26	849.64	3.21	0.999
W15	458	2.29	94.74	0.1	2.97	−49.9	5.6	−179.5	−0.6	0.98	947.40	3.04	0.999
W16	485	9.32	86.95	0.08	3.72	−51.7	5.1	−198.4	−0.5	1.54	1086.88	4.10	0.999
W17	481	2.93	90.42	0.09	6.65	−51.6	4.6	−206	−0.7	1.26	1004.67	6.85	0.999
W18	297.46	3.37	91.77	0	4.86	−63.9	−8.9	−267.7			9177.00	5.03	1.000
W19	397.13	9.27	84.53	0.07	6.13	−60.9	−6.3	−273.4			1207.57	6.76	0.999
W20	419.61	19.69	75.63	0.07	4.61	−62	−6.7	−277.9			1080.43	5.75	0.999
W21	650.96	3.67	91.39	0.28	4.66	−57.9	−9.8	−278.1			326.39	4.85	0.997
W22	730.76	0.34	96.94	0.37	2.35	−59.3	−18.5	−268.7			262.00	2.37	0.996

Table 2. Statistical Data of Hydrogeological Parameters of Co-produced Water from CBM Wells in the Jiergalangtu Block

well name	major ion content (mg/L)							pH	TDS (mg/L)
	HCO_3^-	Cl^-	SO_4^{2-}	Na^+	K^+	Ca^{2+}	Mg^{2+}		
W1	4808	895	11.6	2203	48	10.3	7.2	8.08	5579.10
W2	2723	219	5.41	1072	20.4	10.2	6.49	8.01	2695.00
W4	2747	289.1	5.75	1091	55.6	30.9	13.3	7.47	2859.15
W5	3185.52	570.88	1.71	1481.9	54.91	21.98	16.43	7.6	3740.57
W6	2722.92	792.85	7.19	1476.88	60.7	24.49	7.08	7.76	3730.65
W7	2684.88	903.97	7.61	1592.4	110.26	1306	8.1	7.88	5270.78
W9	2594.56	370.22	1.41	1176.24	20	22.04	7.55	7.49	2894.74
W10	2710	217	79.9	1127	26.3	23.5	10.8	7.96	2839.50
W11	2854	352	70.1	1202	93.1	24.8	9.63	7.75	3178.63
W12	3873	1042	64.9	2092	40.4	43.6	22.7	7.55	5242.10
W13	2524	389	109	1106	24.6	25.9	10.6	7.68	2927.10
W14	2237	215	83.4	988	27.4	18.1	8.18	7.88	2458.58
W15	2404	235	72.8	1060	19	21.3	8.82	7.7	2618.92
W16	2447	261	63.7	1058	33	25.3	10.5	7.68	2675.00
W17	2801	185	77.5	1134	53	32.7	15.8	7.6	2898.50

cumulative thickness of coal seams is 2.35−211.82 m, with an average of 71.51 m. Among them, the no. IV coal group is the main development target layer, with a thickness of 1.6−244.7 m (avg. 53.75 m), and a burial depth of 9.9−501.91 m (avg. 300.51 m), which is distinguished by low-medium ash, medium sulfur, low-medium phosphorus, medium−high moisture, and high volatilization. The vitrinite reflectance (Ro) of the coal in the study area is 0.29−0.48% (avg. 0.35%), which is typical lignite belonging to representative low-rank coal. The hydrogeological conditions are relatively simple in the Jiergalangtu sag, with weak fault transmissibility and weak aquifer watery. The water barrier between aquifers is distributed stably, which is conducive to the preservation and exploitation of CBM.

3. EXPERIMENTS AND METHODS

In order to investigate the origin and accumulation mechanism of low-rank CBM in the Jiergalangtu block, 22 gas samples were collected from CBM exploration wells in the study area. Except wells of W3, W8, W18, W19, W20, W21, and W22, 15 coproduced water samples were collected. All samples are numbered, sorted, sealed, and sent to the laboratory immediately. This study is based on the analysis of 22 gas samples for gas components, $\delta^{13}C(CH_4)$, $\delta D(CH_4)$, $\delta^{13}C(CO_2)$, $\delta^{15}N$, ^3He, 15 coproduced water samples for water quality analysis, $\delta D(H_2O)$, $\delta^{18}O(H_2O)$, $\delta^{13}C_{DIC}$, ^3H, ^{14}C(Fm), and ^{14}C(BP) (Tables 1−3).

The gas composition was determined according to the Chinese standard DZ/T 0064.74-2021, using a gas chromatograph no. 8546 PE.Clarus600. A MAT-253 gas isotope mass

https://doi.org/10.1021/acsomega.3c08490
ACS Omega 2024, 9, 1827−1837

Table 3. Stable Isotope and Radioisotope Dating Data of Co-Produced Water in the Jiergalangtu Block

well name	stable isotope (‰)			radioisotope		
	δD	$\delta^{18}O$	$\delta^{13}C_{DIC}$ (‰)	^3H(TU)	^{14}C age (BP)	^{14}C(Fm) (%)
W10	−104	−14.3	12.9	8.2 ± 0.8	25,500 ± 450	0.0418 ± 0.0023
W11	−107	−15.6	12.4	1.7 ± 0.6	34,770 ± 1400	0.0132 ± 0.0024
W12	−110	−15.4	15.2	0.6 ± 0.6	>50,000	0.0000 ± 0.0024
W13	−106	−14.6	14.5	<0.5	34,840 ± 1450	0.0131 ± 0.0024
W14	−106	−14.5	13.1	0.8 ± 0.5	39,380 ± 2560	0.0074 ± 0.0024
W15	−106	−14.3	13.8	0.6 ± 0.5	34,940 ± 1470	0.0129 ± 0.0024
W16	−107	−14.4	13.2	<0.5	38,210 ± 2210	0.0086 ± 0.0024
W17	−105	−14.3	12.6	1.2 ± 0.6	33,440 ± 1270	0.0156 ± 0.0024
W1	−110	−15.2	12.4	<1.0	45,240 ± 2250	0.0036 ± 0.0024
W2	−106	−14.6	11.2	<1.0	29,660 ± 330	0.0249 ± 0.0024
W4	−106	−14.3	12.9	<1.0	31,410 ± 410	0.0200 ± 0.0024
W5	−106.1	−13.8				
W6	−107	−15.2				
W7	−109.4	−15.3				

spectrometer was used to test the carbon and hydrogen isotopes of methane based on Chinese standards GB/T 18340.2-2010 and DZ/T 0064.89-2021, respectively. Carbon isotopes of carbon dioxide (CO_2) and nitrogen (N_2) isotopes were determined by a MAT-253 gas isotope mass spectrometer according to Chinese standards DZ/T 0184.17-1997 and CZGC2011-4, respectively. Helium isotopes were measured by a Helix SFT instrument based on the Chinese standard Q/CNNC JB 76-2019 (Table 1).

Coproduced water quality was analyzed in accordance with the Chinese standard MT-T1047-2007, and the anion and cation contents and pH values were obtained by an inductively coupled plasma spectrometer 5110VDV and a digital acidity meter PHS-3C (Table 2). Deuterium, oxygen, and sulfur isotopes were measured by a water isotope analyzer according to Chinese standard JCZX-BZ-002-2015. Tritium isotopes were measured by a ultralow background liquid scintillation spectrometer Quantulus1220 based on Chinese standard DZ/T0064.79-2021. A gas isotope mass spectrometer MAT253 Plus was used to detect dissolved inorganic ^{13}C isotopes by the Chinese standard DZ/T0064.87-2021. The ^{14}C in water samples was determined by the Chinese standard DZ/T0064.88-2021 using the accelerator mass spectrometer NEC1.5SDH-1(Table 3).

4. RESULTS

4.1. Gas Composition. The analytical results of the 22 gas samples from the CBM exploration wells in the Jiergalangtu block are shown in Table 1. The gas is dominated by methane with the content ranging from 74.73 to 94.74% (avg. 88.63%). The contents of heavy-hydrocarbons are very low, 0−0.38% for ethane and propane (avg. 0.1%). The C_1/C_{1-n} ratio is 0.999 to 1.0, and the $C_1/(C_2 + C_3)$ ratio range from 241.84 to 9162 (avg. 2560.69), indicating that CBM in this area is superdry gas.[13,32]

Generally, biological gas is featured by dry gas, so the $C_1/(C_2 + C_3)$ ratio can be preliminarily used to determine the biological gas (1000−4000) and thermogenic gas (<1000).[33] The $C_1/(C_2 + C_3)$ ratio of the coalbed gas is 1000−4000, which mainly contains biological gas near the shallow margin of the Powder River Basin in the United States, while the $C_1/(C_2 + C_3)$ ratio near the central part of the basin is less than 1000, showing the characteristics of secondary biological gas and thermogenic mixture.[8] The ratio of secondary biological gas in the San Juan Basin mainly consists of a dry gas characterized by a C_1/C_{1-n} ratio ranging from 0.77 to 1.0 (Scott et al., 1994).[32] In addition, gas samples of the Surat Basin have a $C_1/(C_2 + C_3)$ ratio of over 1000.[6] In the Jiergalangtu block, 45% of the gas samples have a $C_1/(C_2 + C_3)$ ratio exceeding 1000 and 27% of the samples are close to 1000. The C_1/C_{1-n} and $C_1/(C_2 + C_3)$ ratios demonstrate that CBM in the Jiergalangtu block is probably a biological gas with a small amount of thermogenic gas.

The nitrogen content is the highest among nonhydrocarbon gases which is 1.59−21.56% (avg. 7.56%), which is higher than that in China whose N_2 concentration is less than 2%.[34] N_2 concentrations are inversely proportional to CO_2, which is rare in the absence of secondary alteration (Figure 2). Based on the

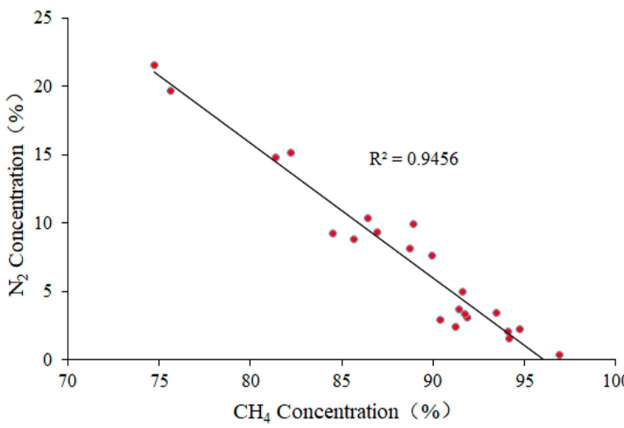

Figure 2. Relationship of CH_4 versus N_2 of CBM in the study area.

above-mentioned, it is indicated that N_2 is mainly of atmospheric origin, which is also demonstrated in the discussion of the N_2 isotope. The surface water carried a large amount of nitrogen and dissolved in it and penetrated into the coalbeds. Therefore, due to the infiltration of N_2 from the atmosphere, the concentration of N_2 and CH_4 presents a negative correlation.

The CO_2 concentration of the gas samples in the study area ranges from 1.17 to 6.65% (avg. 4.00%), which is slightly higher than that in China whose CO_2 concentration is less than 2% (Table 1).[34] However, these data in the Jiergalangtu block are all lower than that of the Powder River Basin (4.9−7%)

https://doi.org/10.1021/acsomega.3c08490
ACS Omega 2024, 9, 1827−1837

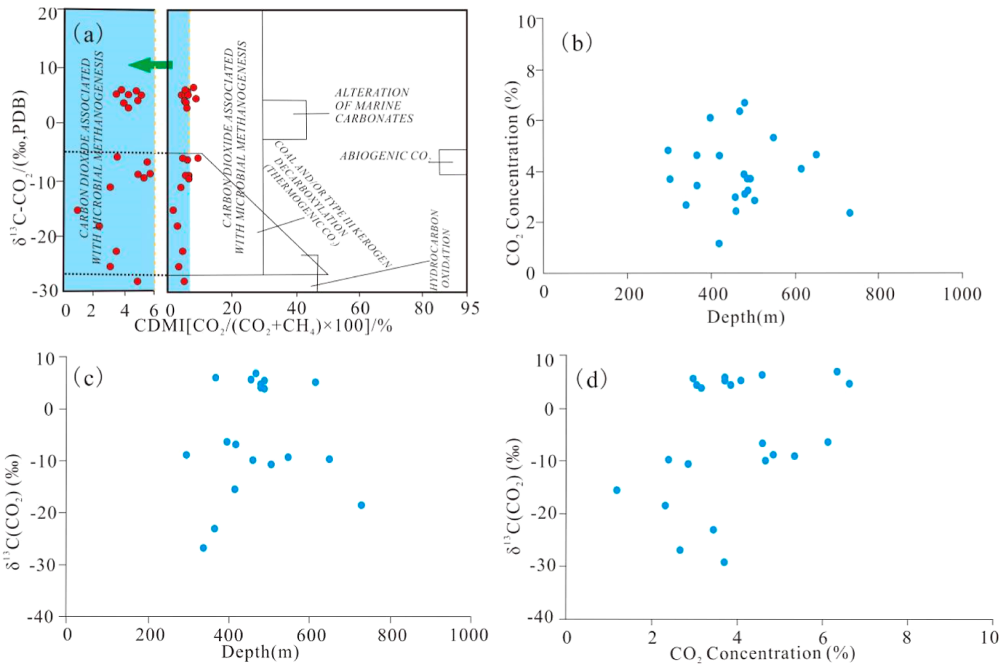

Figure 3. (a) $\delta^{13}C(CO_2)$ versus CDMI for CBM from the Jiergalangtu block, modified from Kotarba and Rice (2001). (b) Relationships of CO_2 versus depth. (c) Scatter diagram of $\delta^{13}C(CO_2)$ versus depth in CBM in the study area. (d) Relationship of CO_2 versus $\delta^{13}C(CO_2)$ in the Jiergalangtu area.

and Sydney and Bowen basins (about 5%).[35] The CO_2 concentration of organic origin is generally less than 15%, and when it reaches more than 60%, most of them tend to be inorganic origin.[36] Therefore, the CO_2 of CBM in the study area can be initially determined to be of organic origin. If the CO_2 of organic origin mainly comes from the coalbeds sand N_2 almost derives from the atmosphere, it can be determined that the CO_2 content in the primitive coalbeds is quite high, while the CH_4 content is much lower. This could deduce that CO_2 may be consumed and converted to other substances, perhaps CH_4 (discussed in detail below).

4.2. Isotopic Characteristics of CBM.

Table 1 gives the analytical results of the carbon, hydrogen, nitrogen, and helium isotopes of 22 gas samples from the produced wells in the Jiergalantu sag.

4.2.1. Carbon and Hydrogen Isotopes in Methane. The $\delta D(CH_4)$ values of gas samples in the Jiergalangtu block range from −278.1 to −173.9‰ (avg. −235.68%) (Table 1). $\delta D(CH_4)$ values have a large distribution interval due to the effects of the degree of thermal evolution and aqueous media. The $\delta D(CH_4)$ values of the biological gas generally change from −400 to −150‰, while that of the secondary biological gas ranges from −225 to +25‰, and the thermogenic gas is not less than −250‰.[3,37,38] Therefore, it is difficult to determine the origin of gas solely based on $\delta D(CH_4)$ values, combined with carbon isotopes, which is required for comprehensive identification.

The distribution of $\delta^{13}C(CH_4)$ values of the gas samples ranges from −68.5 to −48.7‰ (avg. −56.44‰) (Table 1), which is higher than that in the Power River Basin (avg. −68.4‰) and Bowen Basin (avg. −57.10‰). However, it is less than that of the Surat Basin (avg. −51.40‰), the Black Warrior Basin (avg. −51.60‰), and the San Juan Basin (avg. −44.13‰).[6−10] The carbon isotope value of methane is one of the important indexes to decide the CBM origin. Generally, the upper limit of $\delta^{13}C(CH_4)$ value of the biological gas is −55‰; however, due to the influence of secondary biological gas mixing and groundwater dissolution, the value can reach −50‰.[39,40] Approximately 64% of the samples in the Jiergalangtu block have $\delta^{13}C(CH_4)$ values lighter than −55‰, indicating that the majority occur in the biological gas range. Meanwhile, the $\delta^{13}C(CH_4)$ values heavier than −55‰ account for about 36%, exhibiting a small amount, which may be a mixture of biological gas and thermogenic gas.

4.2.2. Carbon Isotopes of the Carbon Dioxide. The $\delta^{13}C(CO_2)$ values of the gas samples in the study area range from −29.4 to 6.8‰ (avg. −5.61‰) (Table 1). Compared with it, the $\delta^{13}C(CO_2)$ values of 165 CBM samples in the Power River Basin range from −24.6 to 22.4‰,[8] and that in the Sydney and Bowen basins is −15.5 to 16.7‰.[35] Therefore, the $\delta^{13}C(CO_2)$ values of the study area are lower than those of the areas mentioned above but most are in the interval. Due to the large isotopic fractionation produced by CO_2 reduction, the $\delta^{13}C(CO_2)$ value associated with secondary biogas varies from −40 to +20‰, and −25 to −5‰ for which thermal degradation of organic matter occurs.[37] The combination of the identification chart of CDMI-$\delta^{13}C(CO_2)$ and the $CO_2/(CO_2 + CH_4)$ (CDMI) values (1.3−6.85%, avg. 4.25%) indicates that CO_2 is primarily an associated product of microbial methanogenesis (Figure 3a).[41] With the increase of burial, the CO_2 content and $\delta^{13}C$ values in the Jiergalangtu block both increase first and then decrease, but there is basically no correlation between them, and both reach the maximum value at the burial of about 450 m (Figure 3b,c). This abnormal enrichment phenomenon is closely related to the biodegradation of original sedimentary organic matter.[42] Due to the preferential consumption of $^{12}C(CO_2)$ by microbial methanogenic bacteria in the process of secondary biogas generation and the differential dissolution of groundwater, the consumption of CO_2 dissolution in a shallower than 450 m burial was higher, and the CO_2 content and $^{13}C(CO_2)$ in a deeper than 450 m burial were greatly affected by isotope

https://doi.org/10.1021/acsomega.3c08490
ACS Omega 2024, 9, 1827−1837

fractionation and microbial secondary transformation, showing a decreasing trend. It is worth noting that the CO_2 content in the study area is not negatively correlated with $\delta^{13}C(CO_2)$ (Figure 3d), that is, the consumption of CO_2 in the biogas production process does not lead to significant enrichment of ^{13}C, which also proves that there are other biogas production pathways in the study area besides CO_2 reduction (as demonstrated in detail below).

4.2.3. Nitrogen Isotopes. There are mainly four sources of N_2 in CBM: atmospheric source, crustal organic origin (produced by organic diagenetic process), crustal inorganic origin (produced by high-temperature metamorphism of nitrogen-bearing rocks in the crust), and degasification source of mantle materials. The isotopic characteristics of N_2 with the four sources are obviously different. The $\delta^{15}N$ from atmospheric sources is +0‰, −2 to +1‰ for mantle material degasification, and N_2 from organic sources is mainly released by microbial ammoniation in the coal immature stage (Ro < 0.6%) with $\delta^{15}N$ less than −10‰.[43]

The $\delta^{15}N$ values of gas samples in the study area range from −3.6 to −0.5‰, and R/R_a values range from 0.03 to 0.15 (mentioned in Section 4.2.4). Combined with the $\delta^{15}N$-R/R_a chart and the concentration correlation of CH_4 and N_2, it can be determined that N_2 is mainly from the atmosphere with a small amount of crustal inorganic origin (Figures 2 and 4).

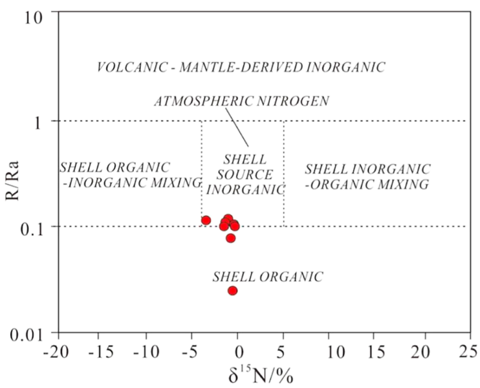

Figure 4. Relationship of $\delta^{15}N$ versus R/R_a. Adapted from ref 43 in accordance with the Creative Commons CC-BY-NC-ND license.

Due to the shallow burial of the coalbeds, N_2 infiltrated the CBM reservoir with atmospheric precipitation during the biogas generation stage. Meanwhile, affected by microbial degradation and secondary biological gas generation, a small quantity of N_2 came from microbial ammonification.

4.2.4. Helium Isotopes. Although the proportion of noble gas in CBM is very small, it brings a lot of geochemical information related to the genesis and evolution of CBM, which could provide important basis for genetic identification of CBM.[42] The end members of $^3He/^4He$ ratios are 1.4×10^{-6}, 2.0×10^{-8}, and 1.1×10^{-5} for the atmospheric source, shell source, and mantle source, respectively.[44] The $^3He/^4He$ ratio in the study area is $(0.42-2.1) \times 10^{-7}$, and 0.03−0.15 for the R/R_a ratio (R is the sample value, and R_a is the atmospheric source value), indicating that helium originates from the atmospheric and earth crust source with no mantle origin (Table 1). Therefore, the $^3He/^4He$ values of the gas samples in the Jiergalangtu block indicate that N_2 has no mantle source, mainly from the atmosphere. CO_2 with higher $\delta^{13}C(CO_2)$ values and lower CDMI values could be the residual materials of microbial reduction and other gas generation pathways, and methane may be a mixture of biological gas and thermogenic gas.

4.3. Geochemical Features of the Coalbed Coproduced Water.

4.3.1. Physicochemical Properties and $\delta D(H_2O)$ and $\delta^{18}O(H_2O)$ Isotopes. As shown in Table 2, the coalbed coproduced water of the Jiergalangtu block shows alkalescency with the pH values, ranging from 7.47 to 8.08 (avg. 7.74). The coalbed water is represented by reducing water dominant in Na, HCO_3, and Cl, with less amount of K, Ca, Mg, SO_4, exhibiting Na−HCO_3 and Na−HCO_3−Cl types. The coalbed water samples have a total dissolved solid (TDS) ranging from 2458.58 to 5579.1 mg/L (avg. 3440.55 mg/L), which is higher than that of the Powder River Basin (avg. 1550 mg/L).[45] Combined with the hydrochemical type and TDS of the coalbed water, it is preliminarily believed that the water environment in the study area is relatively stable, with obvious hydrodynamic stagnation.

The $\delta D(H_2O)$ values of the coalbed produced water change from −110 to −104‰ (avg. −106.82‰), and −15.6 to −13.8‰ (avg. −14.7‰) for the $\delta^{18}O$ values. It can be inferred that the coalbed water do not come from the deeper primitive water whose $\delta^{18}O$ values is higher of 6 to 9‰.[46−48] The δD and $\delta^{18}O$ values of the coproduced water samples are distributed on the local atmospheric precipitation line or near it displayed in the δD and $\delta^{18}O$ identification chart, indicating that most of the aquifers in the study area were mainly supplied by atmospheric precipitation (Figure 5). Small

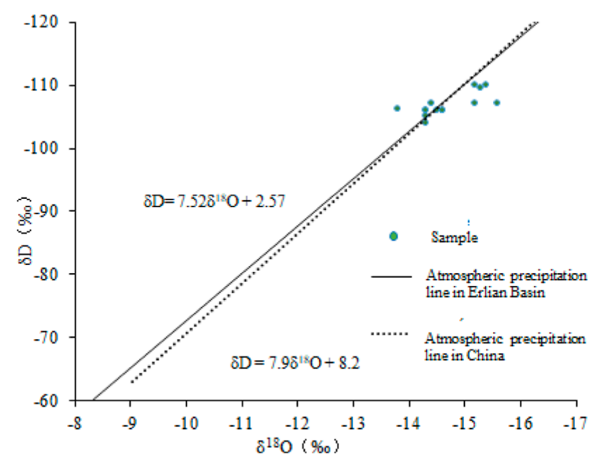

Figure 5. Plot of $\delta D(H_2O)$ values versus $\delta^{18}O(H_2O)$ values of the coproduced water.

samples were located at the upper left of the local precipitation line, indicating that they were weakly affected by atmospheric precipitation evaporation.[45] Therefore, the coal seam water in the study area is mainly derived from atmospheric precipitation, which entered the coalbeds through the surface runoff and was retained for a long time, resulting in the dispersion of δD and $\delta^{18}O$ in the formation water, but the values are on or near the local atmospheric precipitation line on the whole.

4.3.2. Radioisotopes Dating. Table 3 shows that the $\delta^{13}C_{DIC}$ values of the coproduced water in the Jiergalangtu block are all positive values, varying from 11.2 to 15.2‰, combined with the coproduced water type, which indicates that it is mainly affected by microbial methanogenesis.[5] In order to estimate the retention time of the coalbed water, the analysis of the ^3H and ^{14}C radioisotopes was carried out. Most

https://doi.org/10.1021/acsomega.3c08490
ACS Omega 2024, 9, 1827−1837

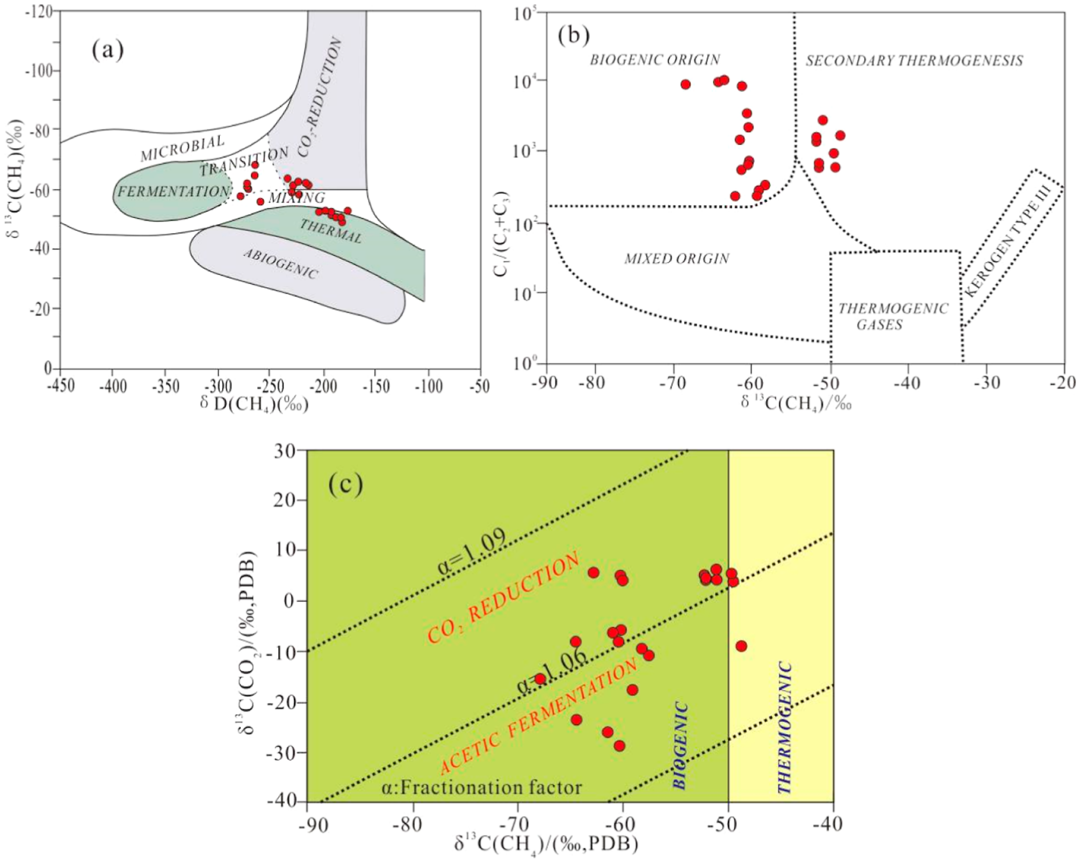

Figure 6. (a) Cross-plot of $\delta^{13}C(CH_4)$ versus $\delta D(CH_4)$ from gas samples. (b) Cross-plot of $C_1/(C_2 + C_3)$ versus $\delta^{13}C(CH_4)$ from gas samples. (c) Diagram showing $\delta^{13}C(CH_4)$ versus $\delta^{13}C(CO_2)$ of 22 gas samples. The plots are fractionation factor lines between CO_2 and CH_4 related to the biological gas origin. Adapted from ref 4 in accordance with the RightsLink Printable License.

of the ^3H values are less than 1.0TU with a few values ranging from 1.2 to 8.2TU, indicating that the coalbed water is a mixture of submodern water and recent recharge water. In other words, there was a small amount of recent recharge water, and most was recharged by submodern water before the year of 1952. Carbon-14 dating is a fairly accurate method. Its range can be traced back thousands of years, and in some cases, it can be detected for more than 50,000 years.[49] The Fm value of ^{14}C modern carbon ratio is 0.0024 to 2.49%, corresponding to the retention time of coproduced water being 25.50−45 millennia, and a few are greater than 50 millennia. This indicates that the age of the coalbed water in the Jiergalangtu block is Quaternary Pleistocene, which further demonstrates that the geological age of the coalbed water is relatively old and less supplied by the present surface water.

5. DISCUSSION

5.1. CBM Genetic Types. This paper combine the most classical Whiticar natural gas genetic identification chart with the latest Milkov natural gas genetic identification chart, based on the former, the CO_2 reduction and methyl-type fermentation pathways can be distinguished, and on account of the latter, the primary biogas and secondary biogas can be identified.[4,50] Based on the interpretation results of $\delta D(CH_4)-\delta^{13}C(CH_4)$ and $\delta^{13}C(CH_4)-C_1/(C_2 + C_3)$ identification chart, biological gas and thermogenic gas are developed in the study area, accounting for 59 and 41%, respectively (Figure 6a,b). The maximum reflectance of vitrinite of coal in the study area is 0.28 to 0.49%, and coal rank in this range can hardly generate thermogenic gas; thus, it is speculated that the "thermogenic gas" here may be secondary biological gas and minor amounts of primary thermal gas. For the isotope separation factor, $\Delta\delta^{13}C(CO_2-CH_4)$ values are 31 to 68.7‰ (avg. 51.82‰) in the study area, approximately 49 to 100‰ and generally distributed between 65−75‰ for the CO_2 reduction pathway, while that of methyl-type fermentation is generally 40 to 55‰.[4] Combined with the separation factor, it can be concluded that 59% of the samples in the study area are of CO_2 reduction, 27% are of methyl-type fermentation, and 14% are of "thermogenesis" (Figure 6c).[40,51]

In order to further identify the primary and secondary biological gas in the study area, the analysis was launched based on the Milkov origin identification diagram. The $\delta^{13}C-CH_4$ and $C_1/(C_2 + C_3)$ values in study area range from −68.5 to −48.7‰ (avg. −56.44‰) and 241.84 to 9162 (avg. 2560.69), respectively, which are both within the range of primary biological gas and secondary biological gas (Figure 7a). CO_2 reduction and methyl-type fermentation are the two major pathways to form biological gas.[8,13] Most of the sample spots distribute in the CO_2 reduction zone, followed by the methyl-type fermentation zone. Furthermore, the analysis is combined with the $\delta D(CH_4)-\delta^{13}C(CH_4)$ and $\delta^{13}C(CO_2)-\delta^{13}C(CH_4)$ identification diagram to distinguish the primary and secondary biological origin. The proportion of secondary biological gas is 40.91 and 59.19% for primary biological gas (Figure 7b,c). Comprehensive analysis of the two types of natural gas identification charts shows that CBM

https://doi.org/10.1021/acsomega.3c08490
ACS Omega 2024, 9, 1827−1837

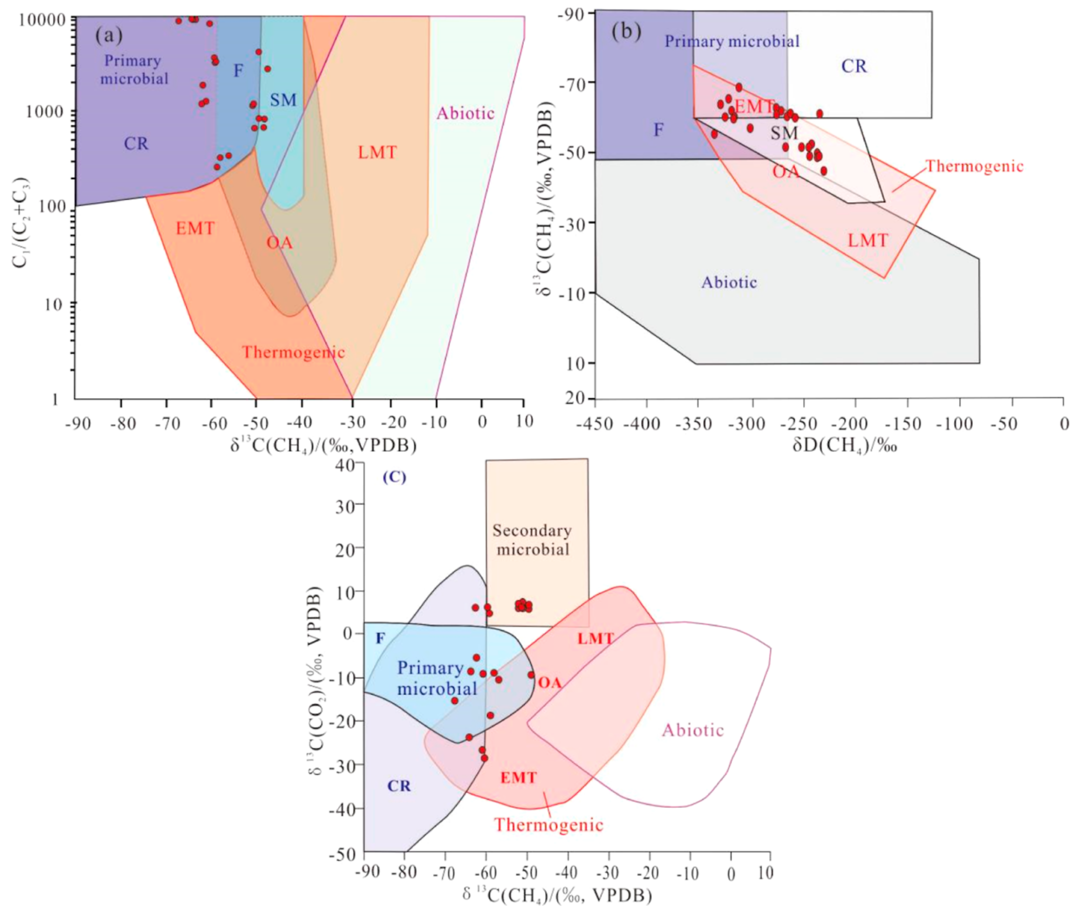

Figure 7. (a) Genetic diagram of $C_1/(C_2 + C_3)$ versus $\delta^{13}C(CH_4)$ from gas samples. (b) Genetic diagram of $\delta^{13}C$ versus δD of methane from gas samples. (c) Genetic diagram of $\delta^{13}C(CO_2)$ versus $\delta^{13}C(CH_4)$ from gas samples (CR-CO_2 reduction, F-methyl-type fermentation, SM-secondary microbial, EMT-early mature thermogenic gas, OA-oil-associated thermogenic gas, and LMT-late mature thermogenic gas). Adapted from ref 50 in accordance with the RightsLink Printable License.

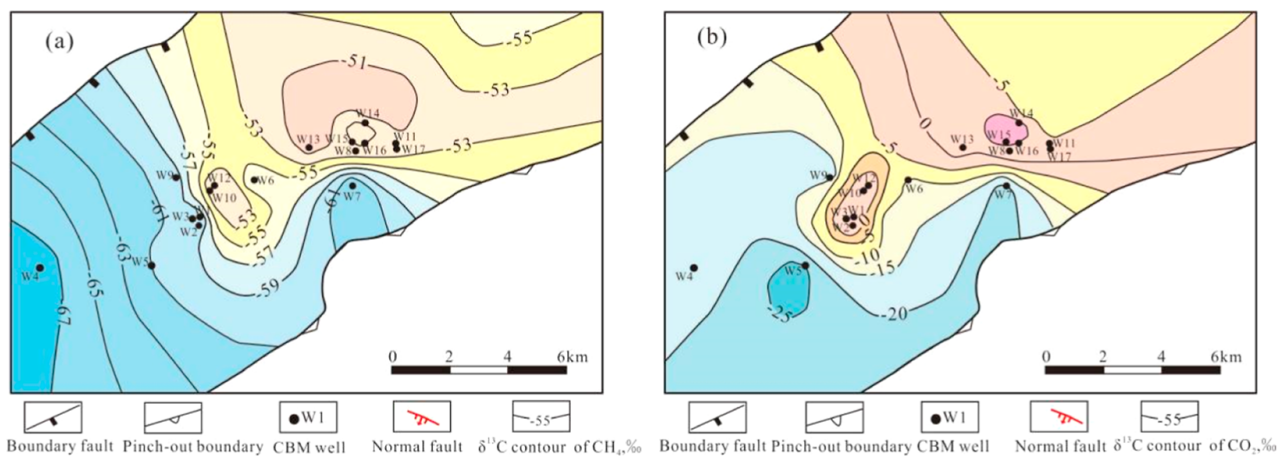

Figure 8. (a) Contour maps of ^{13}C isotopes in methane. (b) Contour maps of ^{13}C isotopes in CO_2.

in the Jiergalangtu block mainly consists of primary biological gas and secondary biological gas, among the biological gas, 31.82% for methyl-type fermentation and 68.18% for CO_2 reduction.

The distribution of high values of carbon isotopes of methane and carbon dioxide is roughly consistent (Figure 8). The higher $\delta^{13}C$ values of the central parts of the block and lower values near the margin of the block indicate that CO_2 reduction occurred continuously in the central parts of the block where CO_2 consumption and ^{13}C enrichment happened. The light $\delta^{13}C$ values at the margin of the block may be affected by methyl-type fermentation (a secondary biological process) in the later stage. The shallow coal seams at the margin of the block was primarily recharged by the surface water, which brought fresh dissolved organic carbon and relevant nutrients and stimulated methyl-type fermentation to generate methane. Dissolved organic carbon in the primordial coal substrate in the deep central part of the block was the only

https://doi.org/10.1021/acsomega.3c08490
ACS Omega 2024, 9, 1827−1837

available nutrient, and CO_2 reduction dominated the methanogenesis.[8,52]

5.2. Gas Reservoir Types. Primary biological gas refers to CBM formed by organic matter deposited at the early stage of coalification (Ro < 0.5%) through CO_2 reduction or methyl-type fermentation.[8,47] Secondary biological gas means the biogas generated by the biodegradation of the coal after a certain thermal evolution, which is uplifted to the shallow strata and re-enters the microbial zone under appropriate conditions.[53] The main difference is that the secondary biological gas has experienced a low thermal maturity stage (0.3% < Ro < 1.5%) and was affected by a variety of reducing bacteria, leading to the relatively complex formation process.[4,33,35]

The vitrinite reflectance (Ro) of the coal in the Jiergalangtu block is 0.29% to 0.48% (average 0.35%), combining with the geochemical characteristics of CBM and the coalbed coproduced water, it can be concluded that sealed primary biological gas and secondary biological gas reservoirs are both developed in the Jiergalangtu block.[54] The main geological evidence is as follows: (1) the high TDS and Na−HCO_3 and Na−HCO_3−Cl types of the coalbed water indicate that the current hydrogeological conditions are hardly conducive to the survival of methanogens and the generation of new secondary biogas. (2) The latest isotopes dating data of the coalbed water [the ^{3}H value is mostly less than 1.0TU, 0.0024% < ^{14}C(Fm value) < 0.0249%] show that the formation water is relatively older and less supplied by current surface water. (3) Carbon dioxide ($\delta^{13}C_{CO_2}$ values are −29.4 to 2.8‰, avg. −5.61‰) was significantly degraded by microorganisms, which is a byproduct of biogas generation. (4) The abnormal high content of N_2 was mainly influenced by the late tectonic uplift. After N_2 and methanogenic bacteria entered the coalbeds with precipitation, a large amount of CO_2 was consumed under the action of microorganisms, and a large amount of N_2 was stored in the gas reservoir, which could indirectly demonstrate that the gas reservoir was in the state of sequestration.

5.3. CBM Accumulation Mechanism. In order to clarify the CBM accumulation mechanism, it is necessary to determine the period when each gas enters the coalbeds. The ^{3}H and ^{14}C isotope analysis has confirmed that the coalbed water in the study area was mainly glacial meltwater formed in the Pleistocene period from 0.0255 to 2.4 Ma. According to the relationship between tectonic evolution and hydrocarbon generation (Figure 9), the CBM accumulation process in the Jiergalangtu block can be divided into four stages. (1) Stage I: microbial gas generation probably began as early as about 97 Ma (early Cretaceous) during the peat deposition period of the Sahantara Formation, which occurred simultaneously with the temperature-induced coal mineralization. In the middle and late Early Cretaceous, when the maximum burial of the Saihantala Formation reached about 1300 m, high thermal conditions promoted the generation of thermogenic gas (thermogenic gas in Figure 6), which reached the peak of gas production and accumulated in the coal reservoirs. (2) Stage II: from the end of the Early Cretaceous to the Neogene, the coal-bearing strata began to uplift and denudate, and part of the coal seams was denuded to the surface and exposed to weathering, resulting in the dissipation of the thermal gas and biological gas generated by the coal seams. (3) Stage III: at the beginning of Neogene, due to the influence of the Himalayan movement, the strata began to subside. In particular, glacial meltwater taking along N_2 and CO_2 infiltrated into the coalbeds on a large scale in the Pleistocene, which was the main formation period of the coalbed water, and a large amount of biological gas tended to generate under suitable conditions. In this period, the CO_2 reduction mainly occurred in the central part of the block, and the methyl-type fermentation primarily happened in the margin.[55] (4) Stage IV: influenced by the arid environment in northwest China, the conditions of less atmospheric precipitation, temperature, TDS, and other factors had hardly been conducive to biological gas generation and tended to stop since Holocene.[56]

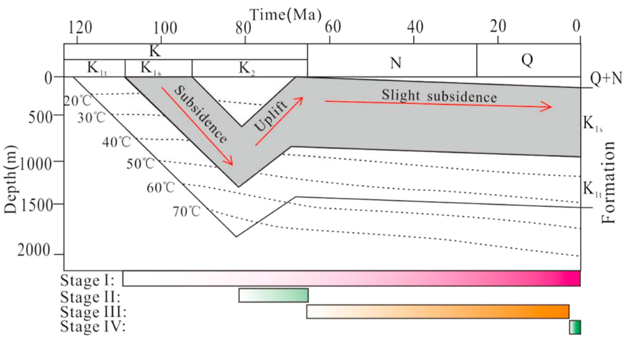

Figure 9. Diagram of coal seam evolution history and accumulation stage in the Jiergalangtu block.

6. CONCLUSIONS

Through comprehensive analysis of gas composition of CBM reservoirs and isotopic characteristics of CBM in the Giergalangtu block, CH_4 is dominated by primary biological gas and secondary biological gas, CO_2 is mainly the associated product of microbial methanogenesis, and N_2 is mainly from atmosphere. Methyl-type fermentation mainly accounted for 31.82% and CO_2 reduction for 68.18%. Constant CO_2 reduction primarily happened with CO_2 consumption and ^{13}C accumulation occurring in the central part of the block, while the light δ^{13}C value at the margin of the block may be influenced by late methyl-type fermentation.

Combined with $\delta D(H_2O)$ and $\delta^{18}O(H_2O)$ isotopes and radioisotopes dating, it has been concluded that the coalbed coproduced water was formed principally in the Quaternary Pleistocene, with relatively old age, and it was less supplied by the present surface water. According to the relationship between tectonic evolution and hydrocarbon generation, CBM formation can be divided into four stages. Primary biological gas mainly generated in Stage I, while a large amount of secondary biological gas was generated in Stage III. Tectonic uplift or tectonic adjustment mainly occurred in Stage II and Stage IV. Therefore, the gas reservoirs chiefly consist of sealed primary biological gas and secondary biological gas.

■ AUTHOR INFORMATION

Corresponding Author

Dazhen Tang − *School of Energy Resources, China University of Geosciences (Beijing), Beijing 100083, China; Coal Reservoir Laboratory of National Engineering Research Center of CBM Development & Utilization, China University of Geosciences, Beijing 100083, China;* orcid.org/0009-0007-0133-5266; Email: tang@cugb.edu.cn

https://doi.org/10.1021/acsomega.3c08490
ACS Omega 2024, 9, 1827−1837

Authors

Ling Li − *School of Energy Resources, China University of Geosciences (Beijing), Beijing 100083, China; Coal Reservoir Laboratory of National Engineering Research Center of CBM Development & Utilization, China University of Geosciences, Beijing 100083, China*

Hao Xu − *School of Energy Resources, China University of Geosciences (Beijing), Beijing 100083, China; Coal Reservoir Laboratory of National Engineering Research Center of CBM Development & Utilization, China University of Geosciences, Beijing 100083, China*

Qin Meng − *Inner Mongolia Coal Exploration Unconventional Energy Co., Ltd., Hohhot 010010, China; Inner Mongolia Coal Exploration New Energy Development Co., Ltd., Hohhot 010010, China; Engineering Technology Research Center of Unconventional Gas of Inner Mongolia Autonomous Region, Hohhot, Inner Mongolia 010010, China*

Haitao Lin − *Inner Mongolia Coal Exploration Unconventional Energy Co., Ltd., Hohhot 010010, China; Inner Mongolia Coal Exploration New Energy Development Co., Ltd., Hohhot 010010, China; Engineering Technology Research Center of Unconventional Gas of Inner Mongolia Autonomous Region, Hohhot, Inner Mongolia 010010, China*

Haipeng Yao − *Inner Mongolia Coal Exploration Unconventional Energy Co., Ltd., Hohhot 010010, China; Inner Mongolia Coal Exploration New Energy Development Co., Ltd., Hohhot 010010, China; Engineering Technology Research Center of Unconventional Gas of Inner Mongolia Autonomous Region, Hohhot, Inner Mongolia 010010, China*

Complete contact information is available at:
https://pubs.acs.org/10.1021/acsomega.3c08490

Author Contributions

All authors contributed to the study conception and contents. Formal analysis, methodology, and writing original draft were performed by Ling Li. Methodology and writing—review and editing were performed by Dazhen Tang. Investigation and writing—review and editing were performed by Hao Xu. Resources, validation, and supervision were performed by Meng Qin, Haitao Lin, and Haipeng Yao. The first draft of the manuscript was written by Ling Li, and all authors commented on previous versions of the manuscript. All authors read and approved the final manuscript.

Notes

The authors declare no competing financial interest.

■ ACKNOWLEDGMENTS

This work was supported by the "14th Five-Year Plan" Forward-Looking Fundamental Major Science and Technology Project of Petrochina Company Limited (subject number: 2021DJ2303) and the Central Guide Local Science and Technology Development Fund project (project number: 2022ZY0018). The authors are grateful to the anonymous reviewers for their careful reviews and detailed comments.

■ REFERENCES

(1) Li, Y.; Pan, S.; Ning, S.; Shao, L.; Jing, Z.; Wang, Z. Coal measure metallogeny: Metallogenic system and implication for resource and environment. *Sci. China Earth Sci.* **2022**, *65* (7), 1211−1228.

(2) Li, Y.; Tang, D. Z.; Fang, Y.; Xu, H.; Meng, Y. J. Distribution of stable carbon isotope in coalbed methane from the east margin of Ordos Basin. *Sci. China Earth Sci.* **2014**, *57* (8), 1741−1748.

(3) Rice, D. D. Composition and Origins of Coalbed Gas. AAPG Special Publication. *Hydrocarbons From Coal*; American Association of Petroleum Geologists, 1993; Vol. *38*, pp 159−184.

(4) Whiticar, J. Carbon and hydrogen isotope systematics of bacterial formation and oxidation of methane. *Chem. Geol.* **1999**, *161* (1−3), 291−314.

(5) Baublys, K. A.; Hamilton, S. K.; Golding, S. D.; Vink, S.; Esterle, J. Microbial Controls on the Origin and Evolution of Coal Seam Gases and Production Waters of the Walloon Subgroup; Surat Basin, Australia. *Int. J. Coal Geol.* **2015**, *147*−*148*, 85−104.

(6) Hamilton, S. K.; Golding, S. D.; Baublys, K. A.; Esterle, J. S. Stable Isotopic and Molecular Composition of Desorbed Coal Seam Gases from the Walloon Subgroup, Eastern Surat Basin, Australia. *Int. J. Coal Geol.* **2014**, *122* (1), 21−36.

(7) Kinnon, E. C. P.; Golding, S. D.; Boreham, C. J.; Baublys, K. A.; Esterle, J. S. Stable isotope and water quality analysis of coal bed methane production waters and gases from the Bowen Basin, Australia. *Int. J. Coal Geol.* **2010**, *82* (3−4), 219−231.

(8) Flores, R. M.; Rice, C. A.; Stricker, G. D.; Warden, A.; Ellis, M. S. Methanogenic Pathways of Coal-Bed Gas in the Powder River Basin,United States:the Geologic Factor. *Int. J. Coal Geol.* **2008**, *76* (1−2), 52−75.

(9) Formolo, M.; Martini, A.; Petsch, S. Biodegradation of Sedimentary Organic Matter Associated with Coalbed Methane in the Powder River and San Juan Basins, U.S.A. *Int. J. Coal Geol.* **2008**, *76*, 86−97.

(10) Pashin, J. C.; Mcintyre-redden, M. R.; Mann, S. D.; Kopaska-Merkel, D. C.; Varonka, M.; Orem, W. Relationships between Water and Gas Chemistry in Mature Coalbed Methane Reservoirs of the Black Warrior Basin. *Int. J. Coal Geol.* **2014**, *126*, 92−105.

(11) Liu, K.; et al. Formation Mechanism of Coalbed Methane in Dafosi Mine Field, HuanGlong Coalfield. *Coal Geol. Explor.* **2022**, *50* (11), 115−124.

(12) Tang, S.; et al. Research Progress of Multi-Source and Multi-Stage Genesis of CO2 -Enriched CBM and the Enlightenments for its Exploration and Development. *Coal Geol. Explor.* **2022**, *50* (3), 58−68.

(13) Tao, M. X. Research Status and Development Trend of Coalbed Methane Geochemistry. *Adv. Nat. Sci.* **2005**, *6*, 648−652.

(14) Zhang, X. J.; Tao, M. X.; Ma, J. L.; Wang, W. C.; Sun, G. Q. Characteristics of Carbon Isotope Composition from Secondary Biogenic Gas in Coalbed Gases:Taking the Huainan Coal Field as an Example. *Pet. Geol. Exp.* **2009**, *31* (6), 622−626.

(15) Yun, J.; Xu, F.; Zeng, W.; Zhong, N. N.; Wang, J. L. Analysis of Critical Restricting Factors and Proposals for Coabed Methane Development in China. *Adv. Mater. Res.* **2011**, *361*−*363*, 848−852.

(16) Li, X.; Fu, X. H.; Liu, A. H.; An, H.; Wang, G.; Yang, X. S.; Wang, L. J.; Wang, H. Methane Adsorption Characteristics and Adsorbed Gas Content of Low-Rank Coal in China. *Energy Fuels* **2016**, *30* (5), 3840−3848.

(17) Ramanathan, V.; Boskovic, D.; Zhmodik, A.; Li, Q.; Ansarizadeh, M. Back to the Future: Shale 2.0-Returning Back to Engineering and Modelling Hydraulic Fractures in Unconventionals with New Seismic to Stimulation Workflows. *SPE/CSUR Unconventional Resources Conference-Canada, September 2014*: Calgary, Alberta, Canada, 2007.

(18) Tao, M. X.; Wang, W. C.; Li, Z. P.; Ma, Y.; Li, J.; Li, X. Comprehensive Study on Genetic Pathways and Parent Materials of Secondary Biogenic Gas in Coalbeds. *Chin. Sci. Bull.* **2014**, *59* (10), 992−1001.

(19) Sun, B.; Shao, L.; Zhao, Q.; Hu, Q. Reservoiring Mechanism of Coalbed Methane and Exploration Direction in Hailaer Basin. *Nat. Gas. Ind.* **2007**, *27* (7), 12.

(20) Xu, F.; Yan, X.; Lin, Z.; Li, S.; Xiong, X.; Yan, D.; Wang, H.; Zhang, S.; Xu, B.; Ma, X.; Bai, N.; Mei, Y. Research Progress and Development Direction Of Key Technologies for Efficient Coalbed Methane Development in China. *Coal Geol. Explor.* **2022**, *50* (3), 1−14.

(21) Ye, J..; Hou, S.; Zhang, S. Progress of coalbed methane exploration and development in China during the 13th Five-Year Plan period and the next exploration direction. *Coal Geol. Explor.* **2022**, *50* (3), 15−22.
(22) Men, X. Y.; Lou, Y.; Wang, Y. B.; Wang, Y. Z.; Wang, L. X. Development Achievements of China's CBM Industry Since the 13th Five-Year Plan and Suggestions. *Nat. Gas. Ind.* **2022**, *42* (6), 173−178.
(23) Sun, F.; et al. Low-Rank Coalbed Methane Exploration in Jiergalangtu Sag, Erlian Basin. *Acta Pet. Sin.* **2017**, *38* (5), 485−492.
(24) Wang, S.; Shao, L.; et al. Characteristics of CBM Reservoirs and Exploration Potential in Jiergalangtu Sag of Erlian Basin. *Coal Geol. Explor.* **2017**, *45* (4), 63−69.
(25) Wang, T.; et al. Evaluation of Coal Reservoir Property and Favorable Area of Coalbed Methane Resources in Jiergalangtu Depression of Erlian Basin. *Saf. Coal Mine* **2020**, *51* (9), 187−191.
(26) Zhang, T. *Geological Characteristics of low-rank CBM and Optimum Selection of Development Blocks of Key Depression in Erlian Basin*; Xuzhou: China University of Mining and Technology, 2019.
(27) Chen, Y. P.; Chen, X. Y.; Yang, J. S.; Chen, S. S.; Dong, Z.; Li, G. Micropore Development Characteristics of Low Coal Rank Reservoirs in Jiergalangtu Depression. *Proceedings of the 2018 National CBM Academic Conference*; Petroleum Industry Press, 2018; pp 191−197.
(28) Wang, G.; Wang, M. J.; Liu, Z.; Zhang, Y. P.; Chen, Y. J.; Ji, T. Geological Characteristics and Reservoir-Forming Regularity of Low-Rank Coalbed Methane in Jiergalangtu Depression. *Proceedings of the 2021 CBM Symposium*; China Economic Publishing House, 2021; pp 197−206.
(29) Sun, Q.; Wang, S. W.; Tian, W. G.; Sun, B.; Chen, J.; Yang, Q.; Chen, H.; Yang, F.; Qi, L. Accumulation patterns of low-rank coalbed methane gas in the Jiergalangtu Sag of the Erlian Basin. *Nat. Gas. Ind.* **2018**, *38* (04), 59−66.
(30) Chen, H.; Qin, Y.; Deng, Z.; Geng, M.; Li, G.; Sang, G. J.; Xia, D. Factors influencing the biogenic gas production of low rank coal beds in the Jiergalangtu sag, Erlian Basin. *Nat. Gas Ind.* **2019**, *6* (06), 1−6.
(31) Tao, J.; Shen, J.; Wang, J.; Li, Y.; Li, C. Genetic Types and Exploration Prospect of Coalbed Methane in Jiergalangtu Depression, Erlian Basin. *Geol. J. China Univ.* **2019**, *25* (2), 295−301.
(32) Scott, A. R.; Kaiser, W. R.; Ayers, W. B., Jr. Thermogenic and Secondary Biogenic Gases San Juan Basin, Colorado and New Mexico-Implications for Coalbed Gas Producibility. *AAPG Bull.* **1994**, *78* (8), 1186−1209.
(33) Golding, S. D.; Boreham, C. J.; Esterle, J. S. Stable Isotope Geochemistry of Coal Bed and Shale Gas and Related Production Waters: a Review. *Int. J. Coal Geol.* **2013**, *120*, 24−40.
(34) Song, Y.; Liu, S.; et al. Geochemical Characteristics and Genesis of Coalbed Methane in China. *Acta Pet. Sin.* **2012**, *33* (s1), 99−106.
(35) Ahmed, M.; Smith, J. M. Biogenic Methane Generation in the Degradation of Eastern Australian Permian Coals. *Org. Geochem.* **2001**, *32*, 809−816.
(36) Dai, J.; Shi, X.; Wei, Y. Summary of the Inorganic Origin Theory and the Abiogenic Gas Pools(Fields). *Acta Pet. Sin.* **2001**, *22* (6), 5−10.
(37) Whiticar, M. J.; Faber, E.; Schoell, M. Biogenic Methane Formation in Marine and Freshwater Environments: CO_2 Reduction VS. Acetate Fermentation-Isotope Evidence. *Geochim. Cosmochim. Acta* **1986**, *50* (5), 693−709.
(38) Song, Y.; Liu, S. B.; Zhang, Q.; Tao, M.; Zhao, M.; Hong, F. Coalbed Methane Genesis,Occurrence and Accumulation in China. *Petrol. Sci.* **2012**, *9* (3), 269−280.
(39) Dai, J. X.; Xia, X. Y.; Qin, S. F.; Zhao, J. Causation of Partly Reversed Orders δ^{13}C in Biogenic Alkane Gas in China. *Oil Gas Geol.* **2003**, *24* (1), 1−6.
(40) Qin, S.; Tang, X.; Song, Y.; Wang, H. Distribution and Fractionation Mechanism of Stable Carbon Isotope of Coalbed Methane. *Sci. China Earth Sci.* **2006**, *49* (12), 1252.
(41) Kotarba, M. J.; Rice, D. D. Composition and Origin of Coalbed Gases in the Lower Silesian Basin, Southwest Poland. *Appl. Geochem.* **2001**, *16*, 895−910.
(42) Ju, Y.-W.; Li, Q.-G.; Yan, Z.-F.; Sun, Y.; Bao, Y. Origin Types of CBM and Their Geochemical Research Progress. *J. China Coal Soc.* **2014**, *39* (5), 806−815.
(43) Li, J.; Li, Z. S.; Wang, X. B.; Wang, D. L.; Xie, Z. Y.; Li, J.; Wang, Y. F.; Han, Z. X.; Ma, C. H.; Wang, Z. H.; Cui, H. Y.; Wang, R.; Hao, A. S. New indexes and charts for genesis identification of multiple natural gases. *Petrol. Explor. Dev.* **2017**, *44* (4), 535−543.
(44) Peters, K. E.; Walters, C. C.; Moldowan, J. M. *The Biomarker Guide:Volume2, Biomarkers and Isotopes in Petroleum Systems and Earth History*; UK:Cambridge University Press, 2005; pp 476−708.
(45) Rice, C. A.; Flores, R. M.; Stricker, G. D.; Ellis, M. S. Chemical and Stable Isotopic Evidence for Water/Rock Interaction and Biogenic Origin of Coalbed Methane, Fort Union Formation, Powder River Basin, Wyoming and Montana U.S.A. *Int. J. Coal Geol.* **2008**, *76*, 76−85.
(46) Martini, A. M.; Walter, L. M.; Budai, J. M.; Ku, T. C. M.; Kaiser, C. J.; Schoell, M. Genetic and Temporal Relations between Formation Waters and Biogenic Methane: Upper Devonian Antrim Shale, Michigan Basin,USA. *Geochim. Cosmochim. Acta* **1998**, *62* (10), 1699−1720.
(47) Strąpoć, D.; Mastalerz, M.; Dawson, K.; Macalady, J.; Callaghan, A. V.; Wawrik, B.; Turich, C.; Ashby, M. Biogeochemistry of Microbial Coal-Bed Methane. *Annu. Rev.* **2011**, *39*, 617−656.
(48) Song, P.; et al. Groundwater Types and Water Source Discriminantion for Xinzheng Mining Area. *Saf. Coal Mine* **2014**, *45* (2), 165−168.
(49) Ma, X.; Song, Y.; Liu, S. B.; Jiang, L.; Hong, F. Origin and Evolution of Waters in the Hancheng Coal Seams, the Ordos Basin, as Revealed from Water Chemistry and Isotope (H, O,129I) Analyses. *Sci. China* **2013**, *56* (11), 1962−1970.
(50) Milkov, A. V.; Etiope, G. Revised Genetic Diagrams for Natural Gases based on a Global Dataset of > 20,000 Samples. *Org. Geochem.* **2018**, *125*, 109−120.
(51) Jenden, P. D.; Kaplan, I. R. Comparison of Microbial Gases from the Middle America Trench and Scripps Submarine Canyon: Implications for The Origin Of Natural Gas. *Appl. Geochem.* **1986**, *1* (6), 631−646.
(52) Vinson, D. S.; Blair, N. E.; Martini, A. M.; Larter, S.; Orem, W. H.; McIntosh, J. C. Microbial Methane from in Situ Biodegradation of Coal and Shale: A Review and Reevaluation of Hydrogen and Carbon Isotope Signatures. *Chem. Geol.* **2017**, *453*, 128−145.
(53) Fu, H.; Yan, D.; Su, X.; Wang, J.; Li, Q.; Li, X.; Zhao, W.; Zhang, L.; Wang, X.; Li, Y. Biodegradation of early thermogenic gas and generation of secondary microbial gas in the Tieliekedong region of the northern Tarim Basin, NW China. *Int. J. Coal. Geol.* **2022**, *261*, 104075.
(54) Li, Y.; Fu, H.; Yan, D.; Su, X.; Wang, X.; Zhao, W.; Wang, H.; Wang, G. Effects of simulated surface freshwater environment on in situ microorganisms and their methanogenesis after tectonic uplift of a deep coal seam. *Int. J. Coal. Geol.* **2022**, *257*, 104014.
(55) Fu, H.; Li, Y.; Su, X.; Yan, D.; Yang, S.; Wang, G.; Wang, X.; Zhao, W. Environmental conditions and mechanisms restricting microbial methanogenesis in the Miquan region of the southern Junggar Basin, NW China. *GSA Bulletin* **2023**, *135*, 420−434.
(56) Li, X.; Dong, G. R. Discussion on the Formation Age of Arid Environment in West China. *Quat. Sci.* **2006**, *26* (6), 895−904.

https://doi.org/10.1021/acsomega.3c08490
ACS Omega 2024, 9, 1827−1837